Mechanical and Tribological Properties of the Oxide Thin Films Obtained by Sol-Gel Method

50

Carolina J. Diliegros-Godines, Francisco Javier Flores-Ruiz, Rebeca Castanedo-Pérez, Gerardo Torres-Delgado, and Esteban Broitman

Contents

Abstract

This chapter will discuss the mechanical and tribological stability at the micro- and nanoscales of oxide films deposited by the sol-gel technique. The importance of tribological studies on sol-gel oxide films and of some works available in the literature will be shown. Particularly, films with applications in photovoltaic and photocatalyst devices compound of Cd_2SnO_4 and CdO+$CdTiO_3$ films, respectively, and films obtained from their precursor solutions were evaluated by a

C. J. Diliegros-Godines (✉) · F. J. Flores-Ruiz
CINVESTAV-Unidad Querétaro, Querétaro, Qro, Mexico

CNyN-UNAM, Ensenada, BC, Mexico
e-mail: janani.diliegros@gmail.com

R. Castanedo-Pérez · G. Torres-Delgado
CINVESTAV-Unidad Querétaro, Querétaro, Qro, Mexico

E. Broitman
Thin Film Physics Division, Linköping University, Linköping, Sweden

© Springer International Publishing AG, part of Springer Nature 2018

L. Klein et al. (eds.), *Handbook of Sol-Gel Science and Technology*,
https://doi.org/10.1007/978-3-319-32101-1_115

quantitative novel method for simultaneous in situ measurement of the wear and friction evolution. The results obtained show the microtribological performance of the sol-gel oxides strongly depends on their crystalline phase, microstructure, and synthesis conditions.

Introduction

Nowadays, the industrial market pays attention in the sol-gel technique as a high profitable method to produce oxide films on substrates with large areas or uncommon shapes. Due to the use of oxide films with single- or multilayer configuration in devices as photocatalyst, sensors, solar cells, optical filters, or protective coatings, there is a necessity to have reliable characterization methods in order to guarantee the quality of the films to be used in an industrial level. Since the surface of the devices is usually submitted to handling, and these are exposed to environmental abrasion or wear, changes in the surfaces lead to the loss of both its efficiency and profitability. Thereby, studying the surface mechanical stability of the devices becomes essential. This mechanical stability implies both the study of the mechanical properties of the materials and an analysis of their tribological behavior. However, such studies at nano- or microscales are uncommon for oxide films deposited by the sol-gel technique.

Nanoindentation is perhaps the more relevant technique to study the mechanical properties of oxide films evaluated at the microscale because it is fast and fairly accurate under certain experimental conditions. The technique, originally developed for analyzing indentations in bulk materials, uses the Oliver and Phar method to obtain hardness and elastic modulus from the unloading part of the load–displacement curve (Oliver and Pharr 1992, 2004). If the system consists of substrate coated with a thin film, effects of substrate properties must be taken into account to avoid overestimation or underestimation of the mechanical properties of the film. To avoid this effect, the indentation depth is limited to less than 10% of the film thickness (Pharr and Oliver 1992). However, for films deposited by sol-gel, this limitation is hard to be applied. The thickness of the films is usually less than 100 nm; therefore, some uncertainty appears in the measurement because the nanoindentation is done close to the detection limits. In order to avoid this problem and to obtain reliable values of the film mechanical properties without influence of the substrate, some approximations can be used for indentation depths in the order of the film thickness. However, special care must be taken because these approximations were developed for homogeneous and isotropic materials (Zhou and Prorok 2009, 2011; Han et al. 2011; Li and Vlassak 2011; Li et al. 2011). The evaluation of other mechanical properties, such as residual stress, coating fracture toughness, adhesion, etc., are briefly described in ► Chap. 22, “Low-Temperature Processing of Sol-Gel Thin Films in the SiO_2–TiO_2 Binary System”.

The tribological behavior of oxide films deposited by sol-gel is generally evaluated at the macroscale with the ball on disk configuration, where a ceramic ball is sliding several times on the film surface and the lifetime of the film is evaluated with the number of cycles that the material resist before failure. Under this test, the wear mechanisms are generally evaluated with ex situ observations of wear track through optic or electronic micrographs.

Other test that is commonly used to determine the resistance to scratch of sol-gel oxide films at macroscale is the pencil hardness test, where the value scale ranges from 6B, softest, to 9H, hardest. The value is recorded as the hardest pencil that does not scratch the surface of the coating. However, this test is a qualitative method to determine the hardness. At the microscale, scanning probe microscopy (SPM)-based techniques are used to produce wear and to explore the damage produced during the test (Broitman and Flores-Ruiz 2015; Diliegros-Godines et al. 2015).

The particular interest to study the mechanical properties and tribological behavior of sol-gel oxide films arises, for instance, in solar cells because these devices are subject to handling and packaging during their processing which can lead to surface scratches or delamination, leading to loss of efficiency and decreasing in this manner the estimated lifetime of the solar panel (Diliegros-Godines et al. 2015; Kaule et al. 2014). As well, the mechanical integrity of each one of the oxide layers that constitute the solar cell contributes to the proper operation of the panel. Other examples are the oxides used as protective coatings such as SiO_2, ZrO_2, Al_2O_2, TiO_2, and CeO_2 (Wang and Bierwagen 2009; Figueira et al. 2015). These oxides, under certain experimental conditions of processing, own good chemical stability and mechanical resistance when they are exposed to aggressive environments, which are decisive factors to be used at industrial scale (Wang and Bierwagen 2009). Some reports in the sol-gel literature about mechanical properties and/or tribological behavior will be discussed in the next paragraphs.

Díaz-Parralejo et al. carried out a study by nanoindentation on the mechanical properties of ZrO_2-3 mol%Y_2O_3 (3YZS) deposited by dip-coating sol-gel technique on sapphire substrates as a function of sintering temperature (up to 1500 °C) (Díaz-Parralejo et al. 2010). Their elastic modulus values ($\sim$150 GPa) did not suffer significant changes with variations in the sintering temperature but the hardness values slightly decreased from 8 to 7 GPa for temperatures above 1000 °C. For these films, the grain size presented a greater growth rate than crystallite size. The authors suggested that the growth of the grains took place at the expense of the clustering of the crystallites (Díaz-Parralejo et al. 2010).

Brunckovà et al. studied the substrate influence on the mechanical response of ($K_{0.5}Na_{0.5}NbO_3$, KNN) thin films deposited by spin-coating (Brunckovà et al. 2013). They made use of different approximations to decouple the effective hardness and modulus from the substrate (Zhou and Prorok 2011; Huang and Chang 2010). The calculated KNN film modulus was higher on Pt/Al_2O_3 (91 GPa) than Pt/SiO_2/Si (71 GPa) substrates, which correspond with a much higher elastic modulus of the alumina substrate (double of the SiO_2 modulus). The hardness of the KNN films were approximately the same with a value of 4.5 GPa on both substrates, thus concluding that the influence of substrate on film hardness was insignificant.

Catauro et al. studied Ti-4 disks coated with hybrid ZrO_2-PCL materials synthesized by sol-gel process and deposited by dip-coating in order to improve their wear and corrosion resistance but keeping their biological properties (bioactivity and biocompatibility) (Catauro et al. 2014). They performed scratch tests and showed that the incorporation of PCL decreases the critical load of the films from 7 N for 0 wt.% PCL to ~4 N for 30 wt.% PCL. This decrease was attributed to a lack of homogeneity of the deposited hybrid coatings in presence of a high surface roughness. They concluded that the high tendency to crack of ZrO_2 coatings was decreased with the incorporation of PCL, which also allowed a higher deformation work during scratch test.

Sobczyk-Guzenda et al. studied the mechanical stability of TiO_2 (~250 nm thick) films synthesized by sol-gel to photocatalytic and microbiological applications on stainless steel substrate (Sobczyk-Guzenda et al. 2013). Scratch test with a diamond cone of an apex angle of 90° and a tip curvature <1 μm showed that coating delamination happens at 13 mN critical load. The coating hardness obtained with a Berkovich tip in the continuous stiffness measurement was 0.2 GPa above the substrate (4.6 GPa).

Suriano et al. studied different coatings containing low and high contents of silica as well as a mixed oxide composed of high amount of titania and low amount of silica. The mechanical durability, done by nanoscratch and nanoindentation tests performed by atomic force microscopy (AFM), was compared to a macroscale test (pencil hardness) (Suriano et al. 2015). They observed differences between the nanoscratches obtained on the coatings with a low inorganic fraction and those with high inorganic contents. The coating containing the highest fraction of silica shows a much higher dynamic hardness (nearly 2 GPa) than the other two materials (1 GPa), which have hardness of the same order of magnitude. The results are in agreement with the trend of scratch hardness obtained from pencil tests where samples with a lower inorganic percentage showed hardness of 2B-B and on the opposite shows exceedingly high scratch hardness (7H-8H).

Sol-gel oxide films of more complex system such as Cd_2SnO_4 and $CdTiO_3$, obtained from simple precursor solutions as CdO, TiO_2, and SnO_2, are of interest in different industries. For instance, Cd_2SnO_4 (CTO) films deposited by sol-gel have received great attention in the solar cell technology (Diliegros-Godines et al. 2014a, b, c) because, in addition to their low production costs, the electrical and optical properties for these sol-gel films compete with those deposited by sputtering (Wu 2004). These films have been widely studied in their optical, electrical, and morphological properties. Nevertheless, the tribological behavior is not a usual characterization for these films, even considering that a film mechanical failure could involve a lack of device quality. Studies of nanoindentation have shown that Cd_2SnO_4 films have mechanical properties comparable to indium tin oxide (ITO) films, which are to date the most popular transparent conductive oxide (TCO) but with a high cost of production. Also CTO films, grown by sol-gel, have been applied as a TCO in a Au/Cu_2Te/CdTe/CdS/Cd_2SnO_4/glass solar cell with average efficiency of 10.7% (Diliegros-Godines et al. 2014b). The study of mechanical and tribological behavior in this kind of transparent oxides gives a lot of information about the total efficiency of the solar cells. As another case of study, we have $CdTiO_3$ thin films, which have become a novel material to use as a photocatalyst. The new composite obtained from the mixture of CdO-TiO_2 demonstrates to be highly effective in the degradation of gaseous benzene, in the search of an alternative material to improve the TiO_2 performance (Flores-Ruiz et al. 2016). In the particular case of photocatalytic surfaces, any change in the surface of the films will modify the photocatalytic performance, as was shown for ZnO-SnO_2 films (Torres Martínez et al. 2012). In consequence, these photocatalytic surfaces should be wear resistant for functional applications.

This chapter presents a study on the mechanical stability of transparent Cd_2SnO_4 and photocatalytic $CdTiO_3$ oxide films obtained from their precursor solutions (CdO, TiO_2, and SnO_2) deposited by sol-gel. Mechanical properties and tribological behavior of these films are discussed in terms of the material structure. The evaluation of mechanical properties and tribological behavior was conducted with a SPM-based technique which allow in situ to assess quantitative information of wear rate, wear ratio, friction coefficient, plastic deformation, and elastic recovery.

Experimental

The sol-gel synthesis is the most important step in order to obtain successful films. Depending on the potential use of the films, the main characteristics of them could be the thickness, the transparency in a certain wavelength, the particle scatter, etc. In this way, the precursor, the catalyst, and the solvents used in the solution are very important to obtain the desired film characteristics. In this section, the synthesis of CdO-SnO_2 and CdO-TiO_2 systems will be briefly discussed. Both systems showed good tribological behavior.

Also, the main structural and optical characterization techniques used for Cd_2SnO_4 and $CdTiO_3$ films will be described. Furthermore, the friction coefficient and wear measurements performed for these films will be discussed.

Synthesis of the CdO-SnO_2 System to Produce Cd_2SnO_4 Films

The cadmium stannate precursor solution was obtained from the mixture of cadmium oxide and tin oxide precursor solutions obtained separately. Both precursor solutions were mixed at room temperature with different tin atomic concentration percentage in solution in a range around to stoichiometric of the Cd_2SnO_4. Lactic acid (0.4 mol) was added to the mixture of both solutions in order to obtain a transparent final precursor solution. The tin molar ratio in solution, necessary to obtain Cd_2SnO_4 films, was 29 wt.% (Diliegros-Godines et al. 2014b).

The films were deposited by the multiple-dipping method on commercial glass substrates as is schematized in Fig. 1, 24 h after the preparation of the precursor solution. The withdrawal speed was 2.0 cm/min. All the films were first thermally pretreated at 100 °C and then subjected to a sintering treatment at 550 °C, in both cases in an air atmosphere for 1 h.

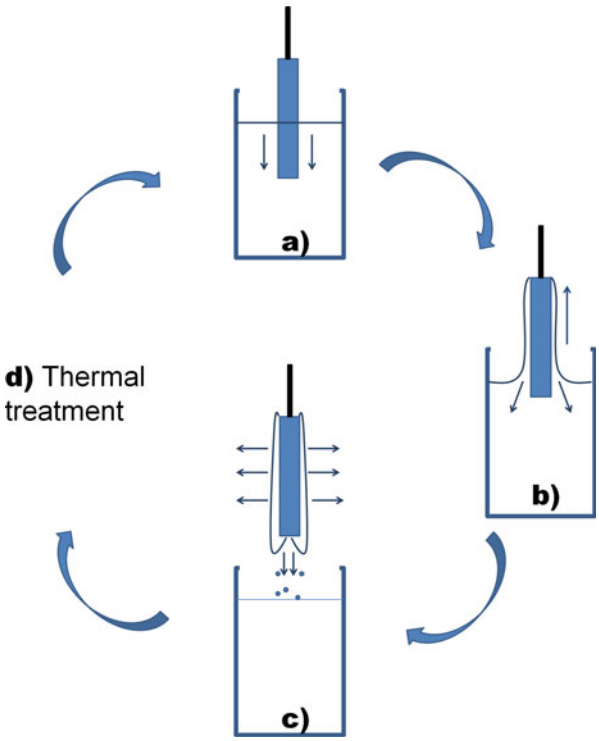

Fig. 1 Multiple-dipping method scheme. (**a**) Immersing of the substrate in the solution; (**b**) the layer is deposited onto the substrate while it is removed from the solution at constant speed, here the speed will determine the thickness of the coating; (**c**) the excess of solution will be drained from the surface, while the solvents (such as alcohols) starts to evaporates from the solution; (**d**) the film is thermally treated to achieve a solid film. The process is repeated n-times depending of the desired final thickness of the film

Synthesis of the TiO_2-CdO System to Produce $CdTiO_3$ Films

The CdO+$CdTiO_3$ films were deposited from the mixture of the cadmium oxide and titanium dioxide precursor solutions obtained separately, as was reported by Hernández et al. (Hernández-García et al. 2015), at different Ti/Cd ratios (0.20, 0.49, 0.65, 0.70, 1). The films were deposited by the multiple-dipping method on commercial glass substrates as is schematized in Fig. 1. CdO and CdO+$CdTiO_3$ films are formed with five coats where each coat was dried and sintered at 100 °C and 490 °C, respectively, both for 1 h.

Structural Characterization of CdO-SnO_2 and TiO_2-CdO Systems

The structural characterization of sol-gel films as CdO, Cd_2SnO_4, TiO_2, and $CdTiO_3$ was conducted by analysis of X-ray diffraction (XRD) patterns in order to identify the crystallographic orientation and crystallite size of the films. Figure 2 shows the XRD pattern of CdO, TiO_2, $CdTiO_3$ (Hernández-García et al. 2015), and Cd_2SnO_4 (Diliegros-Godines et al. 2015) films, where it can be seen that the characteristic diffraction peaks for each crystalline phase.

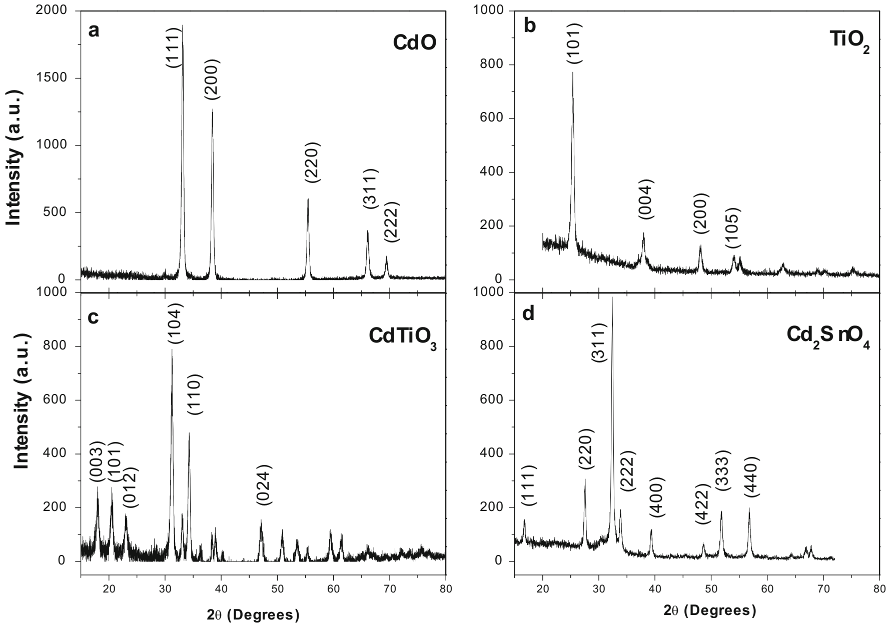

Fig. 2 XRD patterns of (**a**) CdO, (**b**) TiO_2, (**c**) $CdTiO_3$ sol-gel films taken from (Hernández-García et al. 2015) and (**d**) Cd_2SnO_4 sol-gel films taken from (Diliegros-Godines et al. 2015) with patron diffraction file #05-0640, #73-1764, #29-0677 and #34-0928, respectively

Friction Coefficient and Wear Measurements

The microtribological measurements of films from the CdO-TiO_2 (Flores-Ruiz et al. 2016) and CdO-SnO_2 (Diliegros-Godines et al. 2015) systems were performed using a Triboindenter TI 950 from Hysitron with a conical diamond tip (90° opening angle and 5.02 μm nominal tip radius) at a speed of 1 μm/s. The instrument consists of an electrostatic transducer with the capacity to make an indentation followed by a lateral movement on the sample surface while acquiring information of the friction force as a response of the applied force. In this work, a load of 100 μN was used in a reciprocal movement of 31 cycles to obtain information about the evolution of friction and wear. Figure 3 shows a scheme of the procedure to obtain the coefficient of friction and wear profiles. The friction coefficient μ was calculated using $\mu = FF/L$, where FF is the friction force and L is the applied load. The mean contact pressure (Pm) exerted by the indenter on the sample during the experiments was evaluated using Hertz Eq. 1 (Popov 2010). The temperature during the test was around 23 °C and the relative humidity ~50%:

$$Pm = \frac{2}{3}P\max = \frac{2}{3} \cdot \frac{1}{\pi}\left(\frac{6 \cdot L \cdot Er^2}{R^2}\right)^{1/3} \tag{1}$$

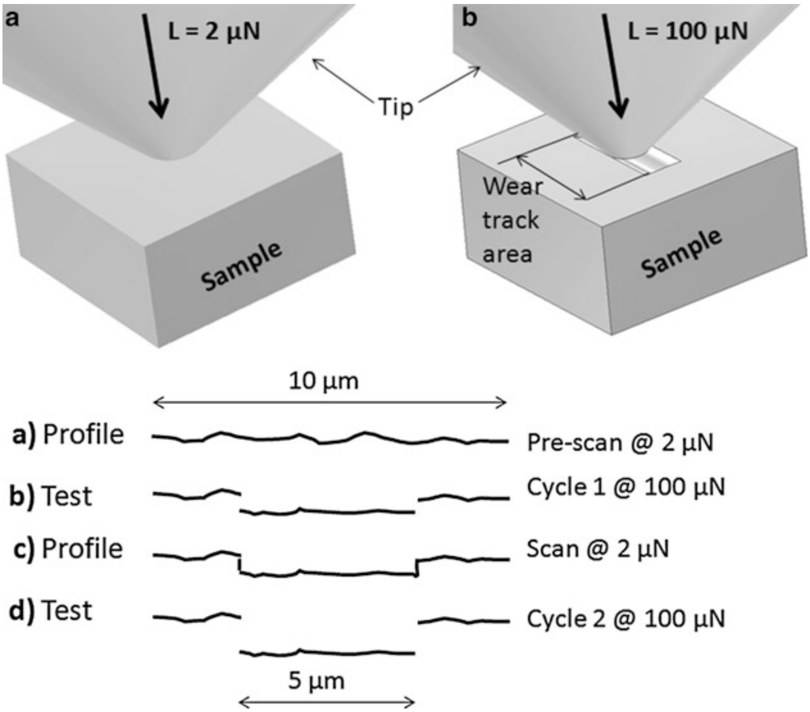

Fig. 3 Schematic of the friction-wear cycles. The information is obtained as follow: (**a**) first, a pre-scan of 10 µm length with a load of 3 µN is made to obtain the topography profile. (**b**) Next, the load is increased to 100 µN and the wear cycle 1 spans 5 µm of length. (**c**) The indenter returns to the base load (3 µN) and a scan of 10 µm length is made to explore the effects of cycle 1. (**d**) After this exploration the load is again applied over the same central line length of 5 µm. Steps (**c**) and (**d**) are repeated 31 times to obtain information about the friction and wear as a functions of the cycles

$Er = \left((1-\upsilon_i{}^2)/E_i + (1-\upsilon_s{}^2)/E_s\right)^{-1}$ is the reduced elastic modulus, E and υ are the elastic modulus and Poisson's ratio for the tip i) and sample (s), R is the tip radius, Pmax is the maximum pressure, and L is the load. Technical details and applications of the measurement method have been published elsewhere (Broitman and Flores-Ruiz 2015; Diliegros-Godines et al. 2015; Broitman et al. 2016).

Results and Discussion

Table 1 summarizes the initial arithmetic average roughness (Ra) of the surface, film thickness, elastic modulus (E), and hardness (H) of the Cd_2SnO_4 and $CdTiO_3$ films and films deposited from their precursor solutions. As mentioned before, Cd_2SnO_4 is used as a transparent conductive oxide for solar cell applications, and their optical

Table 1 Surface roughness and nanomechanical properties of Cd_2SnO_4 (Diliegros-Godines et al. 2015) and $CdTiO_3$ (Flores-Ruiz et al. 2016) systems and their precursor solutions

Sample	Arithmetic roughness (nm)	Film thickness (nm)	Elastic modulus (GPa)	Hardness (GPa)
Cd_2SnO_4	1.40	223.00	88.90	5.70
CdO	15.20	350.00	57.00	1.00
SnO_2	1.00	300.00	99.00	5.90
$CdTiO_3$	5.00	>200.00	37.00	0.85
CdO	8.60	>200.00	22.00	0.25
TiO_2	0.61	>200.00	63.40	1.10
Corning glass-2947	–	–	74.8	6.3

Fig. 4 Wear rate of CdO, TiO_2, $CdTiO_3$ (Flores-Ruiz et al. 2016) and Cd_2SnO_4 (Diliegros-Godines et al. 2015) films deposited on glass substrates by sol-gel

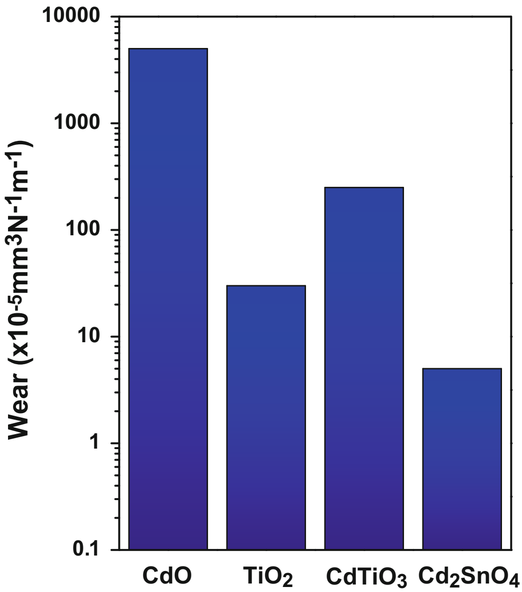

and electrical properties, reported previously by the authors (Diliegros-Godines et al. 2014b), are transmission >85% from 500 to 2600 nm wavelength, resistivity of $\sim 10^{-2}$ Ω cm, and 3.4 eV band gap energy. Resistivity and band gap energy change to 2×10^{-3} Ω cm and 3.58 eV, respectively, when the films are annealed in vacuum at 550 °C for 1 h (see Figs. 4 and 5 in Diliegros-Godines et al. 2014b). On the other hand, photocatalytic films from the $CdTiO_3$ system reported in Hernández-García et al. (2015) have a transmission >70% from 400 to 2000 nm wavelength and band gap energy of 3.4 eV and present a reaction rate constant in degradation of benzene gas with a value of 2.4 h^{-1} which is almost one order of magnitude higher than TiO_2 films.

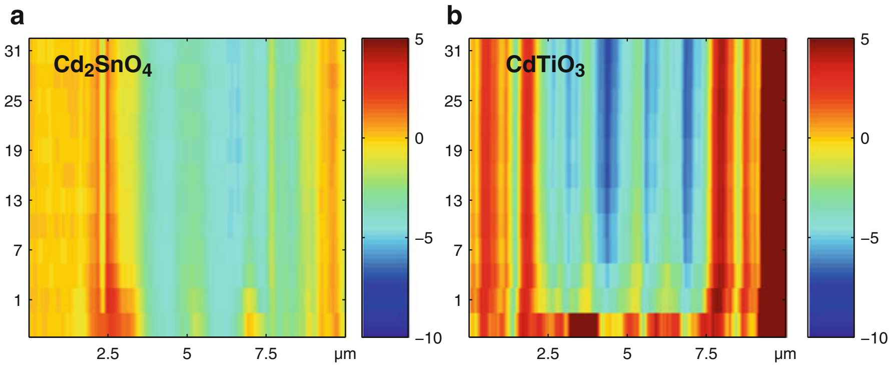

Fig. 5 Wear evolution maps for Cd_2SnO_4 and $CdTiO_3$ film. *Y-axis* indicates the number of cycles to produce wear, *X-axis* is the width of exploration and the *bar scale* represent the wear depth in nanometers. Load of 100 μN were used in both cases to produce wear

Microtribology of CdO-SnO_2 and TiO_2-CdO Systems

The tribological performance of coated system has shown to have a close relationship with the elastic modulus and hardness (Diliegros-Godines et al. 2015; Broitman et al. 2016) (Flores-Ruiz et al. 2014). Films of Cd_2SnO_4 (Diliegros-Godines et al. 2015) and $CdTiO_3$ (Flores-Ruiz et al. 2016) systems and those films obtained from the precursor solutions (CdO, SnO_2, and TiO_2) were analyzed by nanoindentation with penetration depth of ~10% of their total thickness in order to avoid influence from the substrate mechanical properties. Table 1 shows that the Cd_2SnO_4 system had an elastic modulus of 88.9 GPa which is slightly lower than SnO_2 (99 GPa) films but much higher than CdO film (57 GPa). On the other hand, an elastic modulus of 37 GPa was measured for the $CdTiO_3$ system, which is higher than CdO film (22 GPa), but lower than TiO_2 film (63.4 GPa). It can be seen in Table 1 that the measurements of hardness have a similar trend of the elastic modulus.

The XRD patterns in Fig. 2 show that the crystalline phase of each oxide film is reached (as is verified by the PDF-card in Diliegros-Godines et al. 2015; Hernández-García et al. 2015). The result indicates that mechanical properties reported for those films correspond to the single oxide present in the film. Changes in the film composition lead to the presence of additional phases in the oxide films which modifies their mechanical and tribological behavior. For instance, in the case of the Cd_2SnO_4 system, the films that are presenting CdO+Cd_2SnO_4 or Cd_2SnO_4+$CdSnO_3$ phases have poor performance in comparison with the film with single Cd_2SnO_4 phase. The proportion of crystallite from the additional phase has also a strong influence in the mechanical stability. For the CdO+Cd_2SnO_4 film, the proportion of crystallite of the CdO component was higher than Cd_2SnO_4 ones, and its mechanical stability was closed to the CdO film. In the case of the

Cd_2SnO_4+$CdSnO_3$ film, the CdO component is not present and its performance under indentation and friction-wear test was slightly lower than the films with only Cd_2SnO_4 phase.

Although the crystalline phase plays an important role to obtain the desired electrical and optical properties, the film microstructure is another factor to take into account because it provided information about density and type of grown on the substrate, which will influence the mechanical stability and electronic properties of the films (Fattakhova-Rohlfing et al. 2014). Variations in the processing conditions can lead to similar crystalline phases, but with different mechanical response, as the case of CdO films used for the CdO-SnO_2 or TiO_2-CdO systems. CdO film from the CdO-SnO_2 system had an elastic modulus of 57 GPa, while the CdO film from the TiO_2-CdO presents a value of 22 GPa. The main differences in the process of CdO fims in both cases were the number of layers that conforms to the films and the temperature of sintering. In those cases, the microstructure of the films plays an important role in the mechanical properties.

Coated systems, where their surfaces can be under a relative motion or to be susceptible of modifications by the environment of operation, can present a tribological response dependent of the underlying bulk material. For this reason, it is important to know the mechanical properties of the substrate where the films are deposited. The most common substrate used in the sol-gel technique for oxide thin films is Corning glass. In the research discussed in the present work, the sol-gel materials were deposited on Corning glass 2947 substrates. The elastic modulus and hardness evaluated from load–displacement curves were 74.8 and 6.3 GPa, respectively, as indicated in Table 1 (Diliegros-Godines et al. 2015).

The maximum wear rate evaluated during 31 cycles for Cd_2SnO_4, $CdTiO_3$, CdO, and TiO_2 are shown in Fig. 4. Cd_2SnO_4 films have a wear rate (5×10^{-5} mm^3 $N^{-1}m^{-1}$) lower than $CdTiO_3$ films (250×10^{-5} mm^3 $N^{-1}m^{-1}$) and show a close correlation with the hardness and elastic modulus values (see Table 1). The results also show that the wear rate for $CdTiO_3$ is higher than the values for TiO_2 film (30×10^{-5} mm^3 $N^{-1}m^{-1}$ with elastic modulus of 63.4 GPa) and lower than CdO films (5000×10^{-5} mm^3 $N^{-1}m^{-1}$ with elastic modulus of 22 GPa). As it can be reminded, the hardness and elastic modulus for CdO-TiO_2 system shows the same tendency.

Figure 5 shows wear evolution maps obtained during the linear reciprocal test described in the experimental section. The exploration profile shows Ra values of 1.4 and 5.0 nm, and after 31 cycles of wear, these values reach 0.8 and 0.9 nm for Cd_2SnO_4 and $CdTiO_3$, respectively. In the case of friction coefficient, an almost constant value of $\sim$0.48 is observed for Cd_2SnO_4 film and it goes from 0.25 to 0.12 for $CdTiO_3$ film. It can be seen that the wear in Cd_2SnO_4 films is homogeneous throughout test. This reflects the mechanical stability of the film. As well as the $CdTiO_3$ films show a high stability for wear test with a high wear compared with CTO films.

Figure 6 shows the friction coefficient values obtained for CdO, TiO_2, $CdTiO_3$, and Cd_2SnO_4 films. Cd_2SnO_4 films have the highest friction coefficient but the lowest wear rate, and their surface roughness does not change significantly with the

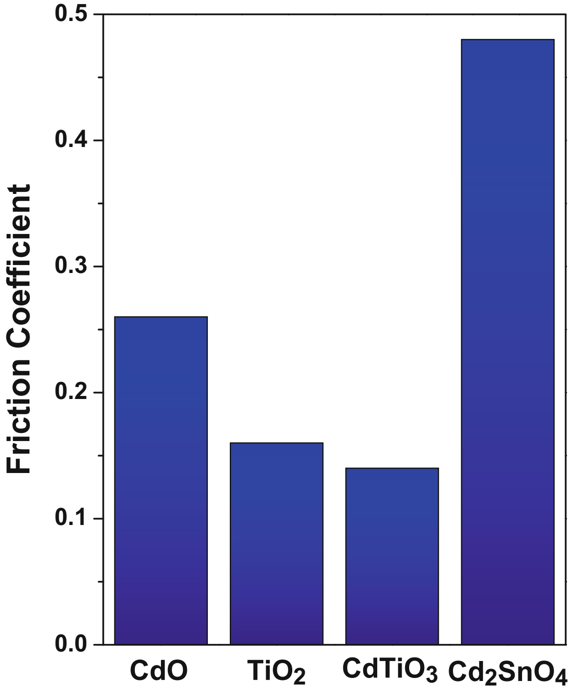

Fig. 6 Friction coefficient values reached during the linear reciprocal test for CdO, TiO_2, $CdTiO_3$ (Flores-Ruiz et al. 2016) and Cd_2SnO_4 (Diliegros-Godines et al. 2015) films deposited by sol-gel on glass substrates

evolution of the test. Also, their mechanical properties are higher in comparison with the $CdTiO_3$ films. $CdTiO_3$ films have the lowest friction coefficient but the resistance to wear and the mechanical properties are lower than Cd_2SnO_4.

Conclusion

This chapter was focused on the mechanical stability of sol-gel oxide thin films at micro- and nanoscales. How an in situ SPM-based technique can be used to assess quantitative information of wear rate, friction coefficient, hardness, and elastic modulus was shown. A complete study of structural and mechanical stability of sol-gel thin films gives information about the performance of the films under environmental abrasion or wear. A brief resume of some reports of tribological behavior and a discussion of the study of two oxides grown by sol-gel were presented. It has been shown that the behavior of the mechanical properties can be related to the following: (i) the technique and parameter of deposition of oxide thin films, (ii) the annealing treatments used to reach a desired crystalline phase or a specific set of properties, and, (iii) in the case of multicomponent oxide films, the presence of each oxide which has an influence on the film microstructure leading to differences in density and stress.

Acknowledgments This work was supported by Consejo Nacional de Ciencia y Tecnología (CONACyT) under Project CeMIE-Sol PY207450/25. The authors would like to thank CONACyT and DGAPA-UNAM for the postdoctoral fellowship awarded to C. J. Diliegros-Godines and F. J. Flores-Ruiz, respectively. The authors also thank to F. A. Hernádez-García for giving some of the samples analyzed in this work. Esteban Broitman acknowledges financial support from the Swedish Government Strategic Research Area in Materials Science on Functional Materials at Linköping University (Faculty Grant SFO Mat LiU No 2009 00971).

References

Broitman E, Flores-Ruiz FJ. Novel method for in-situ and simultaneous nanofriction and nanowear characterization of materials. J Vac Sci Technol A Vac Surf Film. 2015;33:043201. doi:10.1116/1.4921584.

Broitman E, Flores-Ruiz FJ, Di Giulio M, et al. Microstructural, nanomechanical, and microtribological properties of Pb thin films prepared by pulsed laser deposition and thermal evaporation techniques. J Vac Sci Technol A Vac Surf Film. 2016;34:021505. doi:10.1116/1.4936080.

Bruncková H, Medvecký L, Hvizdoš P. Effect of substrate on microstructure and mechanical properties of sol-gel prepared (K, Na)NbO3 thin films. Mater Sci Eng B Solid State Mater Adv Technol. 2013;178:254–62. doi:10.1016/j.mseb.2012.12.003.

Catauro M, Bollino F, Papale F, et al. Corrosion behavior and mechanical properties of bioactive sol-gel coatings on titanium implants. Mater Sci Eng. 2014;43:375–82. doi:10.1016/j.msec.2014.07.044.

Díaz-Parralejo A, Ortiz AL, Caruso R. Effect of sintering temperature on the microstructure and mechanical properties of ZrO2-3 mol%Y2O2 sol-gel films. Ceram Int. 2010;36:2281–6. doi:10.1007/s11106-007-0070-0.

Diliegros Godines CJ, Pérez RC, Delgado GT, Ángel OZ. High transmission and low resistivity cadmium tin oxide thin films deposited by sol-gel. MRS Proc 1675:mrss14–1675–k14–04. 2014a. doi:10.1557/opl.2014.878.

Diliegros Godines CJ, Torres Castanedo CG, Castanedo Pérez R, et al. Transparent conductive thin films of Cd2SnO4 obtained by the sol–gel technique and their use in a solar cell made with CdTe. Sol Energy Mater Sol Cells. 2014b;128:150–5. doi:10.1016/j.solmat.2014.05.023.

Diliegros-Godines CJ, Castanedo-Pérez R, Torres-Delgado G, Zelaya-Ángel O. Structural, electrical and optical properties of tin doped cadmium oxide thin films obtained by sol–gel. J Sol-Gel Sci Technol. 2014c;70:500–5. doi:10.1007/s10971-014-3312-x.

Diliegros-Godines CJ, Flores-Ruiz FJ, Castanedo-Pérez R, et al. Mechanical and tribological properties of CdO + SnO_2 thin films prepared by sol–gel. J Sol-Gel Sci Technol. 2015;74:114–20. doi:10.1007/s10971-014-3584-1.

Fattakhova-Rohlfing D, Zaleska A, Bein T. Three-dimensional titanium dioxide nanomaterials. Chem Rev. 2014;114:9487–558. doi:10.1021/cr500201c.

Figueira RB, Silva CJR, Pereira EV. Organic–inorganic hybrid sol–gel coatings for metal corrosion protection: a review of recent progress. J Coat Technol Res. 2015;12:1–35. doi:10.1007/s11998-014-9595-6.

Flores-Ruiz FJ, Enriquez-Flores CI, Chiñas-Castillo F, Espinoza-Beltrán FJ. Nanotribological performance of fullerene-like carbon nitride films. Appl Surf Sci. 2014;314:193–8. doi:10.1016/j.apsusc.2014.06.168.

Flores-Ruiz FJ, Diliegros Godines CJ, Hernández-García FA, et al. Mechanical and tribological properties of CdO-TiO2 films obtained by sol-gel technique. 2016.

Han SM, Guyer EP, Nix WD. Extracting thin film hardness of extremely compliant films on stiff substrates. Thin Solid Films. 2011;519:3221–4. doi:10.1016/j.tsf.2010.12.167.

Hernández-García FA, Torres-Delgado G, Castanedo-Pérez R, Zelaya-Ángel O. Photodegradation of gaseous C6H6 using CdO + $CdTiO_3$ and TiO_2 thin films obtained by sol–gel technique. J Photochem Photobiol A Chem. 2015;310:52–9. doi:10.1016/j.jphotochem.2015.05.021.

Huang Y, Chang S. Substrate effect on mechanical characterizations of aluminum-doped zinc oxide transparent conducting films. Surf Coat Technol. 2010;204:3147–53. doi:10.1016/j.surfcoat.2010.02.073.

Kaule F, Wang W, Schoenfelder S. Modeling and testing the mechanical strength of solar cells. Sol Energy Mater Sol Cells. 2014;120:441–7. doi:10.1016/j.solmat.2013.06.048.

Li H, Vlassak JJ. Determining the elastic modulus and hardness of an ultra-thin film on a substrate using nanoindentation. J Mater Res. 2011;24:1114–26. doi:10.1557/jmr.2009.0144.

Li H, Randall NX, Vlassak JJ. New methods of analyzing indentation experiments on very thin films. J Mater Res. 2011;25:728–34. doi:10.1557/JMR.2010.0095.

Oliver WC, Pharr GM. An improved technique for determining hardness and elastic modulus using load and displacement sensing indentation experiments. J Mater Res. 1992;7:1564.

Oliver WC, Pharr GM. Measurement of hardness and elastic modulus by instrumented indentation: advances in understanding and refinements to methodology. J Mater Res. 2004;19:3–20. doi:10.1557/jmr.2004.19.1.3.

Pharr G, Oliver W. Measurement of thin film mechanical properties using nanoindentation. Mrs Bull. 1992;17:28–33. doi:10.1557/S0883769400041634.

Popov VL. Rigorous treatment of contact problems-Hertzian contact. In: Popov VL, editor. Contact mechanics and friction. Berlin: Springer; 2010. p. 55–70.

Sobczyk-Guzenda A, Pietrzyk B, Jakubowski W, et al. Mechanical, photocatalytic and microbiological properties of titanium dioxide thin films synthesized with the sol–gel and low temperature plasma deposition techniques. Mater Res Bull. 2013;48:4022–31. doi:10.1016/j.materresbull.2013.06.024.

Suriano R, Oldani V, Bianchi CL, Turri S. AFM nanomechanical properties and durability of new hybrid fluorinated sol-gel coatings. Surf Coat Technol. 2015;264:87–96. doi:10.1016/j.surfcoat.2015.01.015.

Torres Martínez DY, Castanedo Pérez R, Torres Delgado G, Zelaya Ángel O. Structural, morphological, optical and photocatalytic characterization of ZnO–SnO_2 thin films prepared by the sol–gel technique. J Photochem Photobiol A Chem. 2012;235:49–55. doi:10.1016/j.jphotochem.2012.03.009.

Wang D, Bierwagen GP. Sol–gel coatings on metals for corrosion protection. Prog Org Coat. 2009;64:327–38. doi:10.1016/j.porgcoat.2008.08.010.

Wu X. High-efficiency polycrystalline CdTe thin-film solar cells. Sol Energy. 2004;77:803–14. doi:10.1016/j.solener.2004.06.006.

Zhou B, Prorok BC. A discontinuous elastic interface transfer model of thin film nanoindentation. Exp Mech. 2009;50:793–801. doi:10.1007/s11340-009-9309-7.

Zhou B, Prorok BC. A new paradigm in thin film indentation. J Mater Res. 2011;25:1671–8. doi:10.1557/JMR.2010.0228.